Journal of Applied Electrochemistry **31**: 1103–1108, 2001.

Effect of silicon alloying addition on the corrosion behaviour of aluminium in some aqueous media

S.A. SALIH, A.G. GAD-ALLAH, A.A. MAZHAR and R.H. TAMMAM
Chemistry Department, Faculty of Science, Cairo University, Giza, Egypt

Received 10 November 2000; accepted in revised form 29 May 2001

Key words: Al–Si alloy, corrosion, dissolution kinetics, impedance, passivation

Abstract

The corrosion behaviour of three Al–Si alloys was studied after galvanostatic passivation in 0.1 M sodium tartrate, sulfate and borate solutions using EIS techniques. The degree of passivation depends on the anion type, the degree of polarization and the alloy composition. It was also found that increase in pH led to a decrease in polarization resistance R_p. The effect of formation voltage, V_f, on the growth and dissolution kinetics of the oxide grown on the alloys was studied. The polarization resistance value increases as V_f increases up to a certain value; above this the R_p value decreases. This critical V_f depends on the alloy composition and the test solution. The kinetics of oxide layer dissolution in the absence and presence of Cl^- ions was also studied. Increase in immersion time leads to a more severe attack by Cl^- ions as shown by the decrease in the value of R_p. At low Cl^- ion concentration the value of R_p is higher than that in chloride ion free sulfate solutions, because the rate of passive film repair is much higher than that of barrier layer dissolution. However, at high Cl^- ion concentration penetration of Cl^- through defects in the barrier layer leads to formation of an oxyhalide layer.

1. Introduction

Silicon is often added to aluminium to improve its mechanical properties. Studies have been carried out on the electrochemical behaviour of Al and Al–Si alloys in different aqueous media containing different ions by several techniques [1–3]. However, it is clear that relatively little is known about the corrosion of aluminium alloys containing different percentages of Si element below and above the eutectic composition in aqueous media. Such a study will throw light on the optimum Al/Si ratio to give the best electrochemical properties of the alloy.

2. Experimental details

The impedance measurements were carried out using the impedance measurements system (IM6 Zahner electrik, Messtechnik, Germany). Impedance measurements were conducted, with an excitation amplitude of 10 mV peak-to-peak, and a frequency domain from 0.1 Hz to 100 kHz.

The composition of the three Al–Si alloys used in this study are shown in Table 1.

The electrodes were connected to a small copper mould which was fixed in a glass tube with an epoxy adhesive resin (Araldite, Ciba-Production, Switzerland). Only the cross-sectional area of the electrodes were left to contact the test solution. The apparent cross-sectional area of electrode I was 0.525 cm^2, while that of electrodes II and III was 0.55 cm^2.

To achieve high reproducibility, the metal electrodes were pretreated always using the same procedure. The electrodes were mechanically polished with successive grades of emery paper down to 5/0. The final polish was made by rubbing with a fine tissue paper so that the surface was mirror bright. The electrode was then rinsed several times with triply distilled water and immersed directly in the test solution. Solutions used in this work were prepared from AnalaR grade reagents by appropriate dilution. Triple distilled water was used for the preparation of the solutions. Measurements were carried out at constant temperature (25 ± 0.5) °C.

3. Results and discussion

3.1. *Studies on the electrochemical behaviour of anodized Al–Si alloys*

3.1.1. *Effect of anodic polarization on R_p*

The electrode was anodically polarized to 500 or 1000 mV positive to the open circuit potential at a constant current density 10 mA cm^{-2}. The electrode was previously immersed for 2 h in the test solution. This was a 0.1 M solution of sodium sulfate, borate or tartrate of pH 7.0, 9.2 and 4.1, respectively. These

Table 1. Composition of the three Al–Si alloys

	Si	Cu	Zn	Pb	Co	Ni	Fe	Cr	Al
Alloy I	7.0	0.048	0.004	0.001	<0.02	0.023	0.136	0.006	Balance
Alloy II	11.0	0.123	0.014	0.002	<0.05	0.073	0.113	0.025	Balance
Alloy III	22.0	0.282	0.021	0.007	<0.05	0.385	0.179	0.056	Balance

Table 2. R_p values (kΩ cm^2) for the three Al–Si alloys after anodic polarization to 500 or 1000/mV

Salt solution 0.1 M	I		II		III	
	500 mV	1000 mV	500 mV	1000 mV	500 mV	1000 mV
Sulfate	83.7	99.4	105.2	117.9	48.1	52.4
Borate	91.9	163.0	95.6	155.2	96.0	140.6
Tartrate	168.3	212.7	90.0	244.9	82.9	114.9

anions are known to form barrier films on Al when anodically polarized [4]. After 10 min polarization at 500 or 1000 mV anodic to open-circuit potential, the impedance plot was recorded and the polarization resistance, R_p, estimated in each case. The results are shown in Table 2.

The main feature is that R_p is higher on polarizing the electrode to 1000 mV positive to open-circuit conditions as compared to 500 mV, and that both are higher than the value recorded under the same conditions for the electrode at open-circuit potential (i.e., after 2 h immersion in the same medium). Thus, the passivation of the alloy increases as it is polarized to potentials more positive than the open-circuit potential. This has been observed before in the corrosion of Al in acid and neutral media [5]. Thus, anodization leads to formation of more protective oxide films on the alloy surface. The increase in passivation can be explained by a mechanism that includes separation between pitting and corrosion potentials [6] and hence causes an increase in the potential region where the electrode becomes passive. The degree of passivation of any electrode is dependent on both its composition and the anion type present in the test solution. It is well known that well defined barrier oxide films are formed in borate and tartrate solutions [7].

Another feature is that the dependence of the degree of passivation of a certain alloy, on the anions present in the test solution, is complex. The increase in R_p, and hence decrease in capacitance as shown in Table 3, may

Table 3. C_{dl} values (μF cm^{-2}) for the three Al–Si alloys after anodic polarization to 500 or 1000 mV

Salt solution 0.1 M	I		II		III	
	500 mV	1000 mV	500 mV	1000 mV	500 mV	1000 mV
Sulfate	25.3	24.1	24.7	23.8	23.5	22.1
Borate	30.9	28.1	29.4	27.0	26.4	25.1
Tartrate	41.0	40.4	42.7	40.1	39.9	39.1

Table 4. Open-circuit potential (V vs SCE) for the three Al–Si alloys after polarization to 1000 mV

Salt solution	I	II	III
Sulfate	−0.525	−0.510	−0.604
Borate	−0.394	−0.408	−0.492
Tartrate	−1.400	−0.498	−0.473

Table 5. R_p values (kΩ cm^2) of the alloys after polarization to 500 mV in 0.25 M tartrate solution as function of pH

pH	4	6.46	1
Alloy I	–	127	3.5
Alloy II	65.5	91	11.4
Alloy III	–	42	10.5

be due to compositional changes of the oxide film formed. This may result in a decrease in the dielectric constant, as suggested in a previous study [4].

It can be gathered from Tables 2, 3 and 4 that a number of factors are involved in the passivation of the alloys. These are the type of anions in solution, the anodization potential and the alloy composition. The type of anions plays its role through the extent of incorporation inside the barrier oxide layer. This has been suggested in a study dealing with the growth of anodic oxide films on Al in H_2SO_4 [8].

The effect of pH was tested in 0.25 M tartrate solution after polarizing the electrode to 500 mV positive to the open-circuit potential. The results for the three electrodes are given in Table 5. It is clear that the lowest R_p values are obtained in alkaline media. This agrees with the observation [9] that increase in pH from 6.8 to 9.25 led to decrease in oxide film resistance.

3.1.2. *Effect of formation voltage (V_f) on the growth and dissolution kinetics of the oxide grown on the alloys*

Oxide films were formed at a constant current density of 10 mA cm^{-2} up to the required V_f. The impedance plots were recorded to obtain the value of R_p at the instant of immersion in the test solution. In general, the oxide continued to grow with increase in V_f as indicated by increase in the value of R_p. At some positive potential, oxide growth ceased, indicating that a maximum limiting thickness was obtained, dependant on the alloy and medium. At this point, the value of R_p was observed to decrease, indicating breakdown of the formed oxide. The dissolution kinetics were followed by determining R_p values at each V_f for the alloy in the test solution.

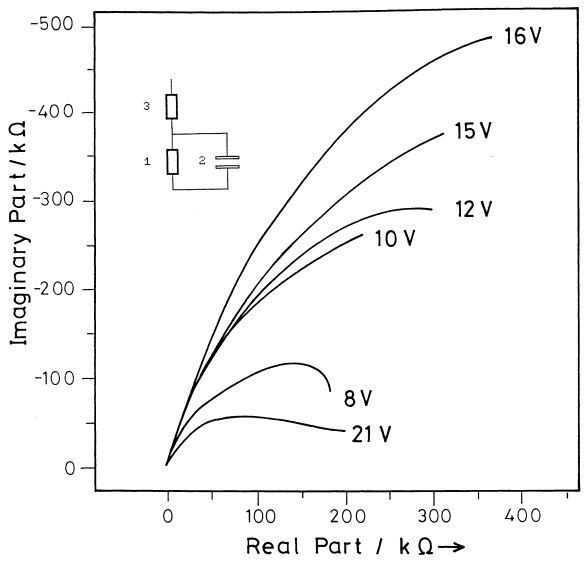

Fig. 1. Nyquist plot and equivalent circuit for alloy III in 0.1 M sulfate solutions at different formation voltages.

As an example, the Nyquist plot for alloy III in 0.1 M sodium sulfate solution is shown in Figure 1. For all formation voltages the system response in the Nyquist complex plane is an incomplete semicircle, whose diameter increases with V_f up to 16 V, then starts to decrease with further increase in V_f. The exact diameter of the depressed semicircle was determined to estimate the value of R_p at each V_f. Due to the rotation of the capacitive semicircle under the real axis, the oxide formed on the alloy cannot be considered to have ideal dielectric properties. This conclusion is supported by the Bode plot, Figure 2, where the phase shift between current and voltage assumes values of about 78°–79°, depending on V_f. This behaviour was related to the nonhomogenity within the oxide film mass [10] and the presence of surface defects in the electrode surface [11], so that the surface is not ideally smooth.

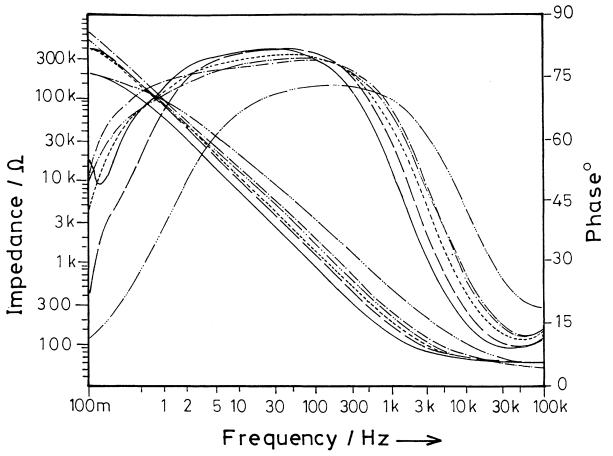

Fig. 2. Bode plot for alloy III in 0.1 M sulfate solutions at different formation voltages. Key (top to bottom curve): (– ··· –) 16 V; (– · – · –) 15 V; (– · · –) 12 V; (----) 10 V; (— —) 8 V; (——) 21 V.

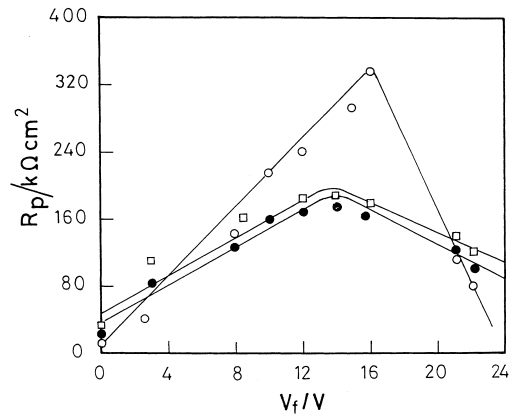

Fig. 3. Dependence of polarization resistance, R_p, on formation voltage, V_f. Key: (□) alloy I; (●) alloy II; (○) alloy III.

The results of R_p determination as a function of V_f for the three alloys in sulfate medium indicate that the oxide continues to grow on the surface of the alloys up to a V_f of 15.0–16.5 V as shown in Figure 3. The Nyquist plot shown in Figure 1 indicates that the capacitive semicircle formed at 16 V is the largest for alloy III, and therefore the oxide formed at this V_f has the most protective properties.

The breakdown voltage, after which R_p starts to decrease is somewhat higher in tartrate than sulfate solutions, for example, 17.5 V in tartrate solution and 15.0 V in sulfate solution for alloy II.

The barrier film thickness, d, was calculated at each V_f using the following relation:

$$C = \varepsilon\varepsilon_0/d \tag{1}$$

where ε_0 is the permittivity of free space (8.85×10^{-12} F m^{-1}) and ε is the dielectric constant of the oxide ($\varepsilon = 10$ for Al_2O_3 [12]) and d is the thickness of the oxide layer. Although the dielectric constant may have a value different from that reported for Al_2O_3 due to the presence of Si in the alloy, this difference will not affect the trend obtained. Assuming the double layer capacitance, C_{dl}, to be much higher than C_{ox}, its effect on the

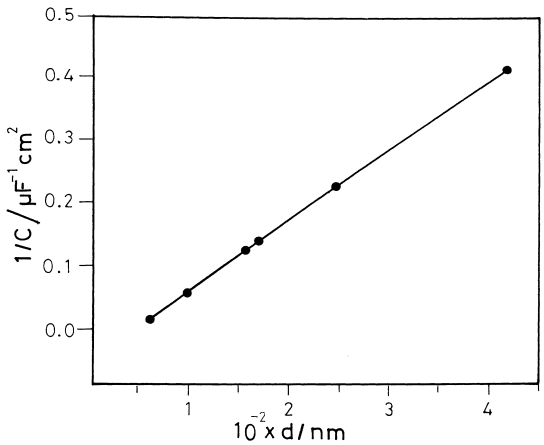

Fig. 4. Relation between $1/C$ against d for alloy I in tartrate solutions at different V_f.

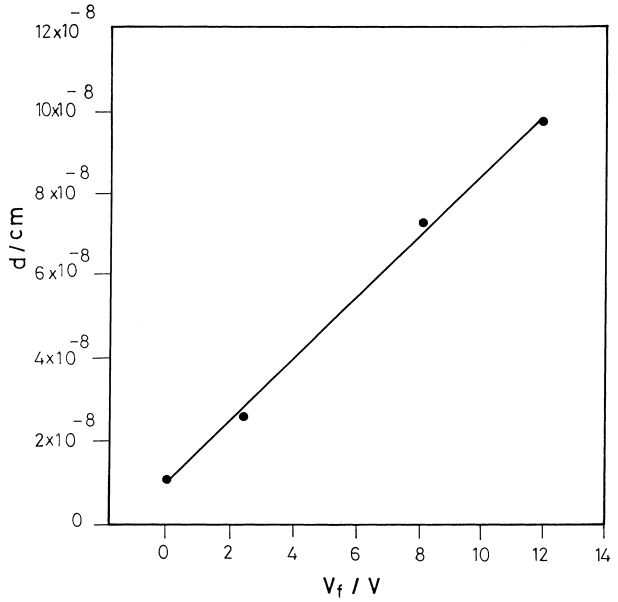

Fig. 5. Relation between oxide thickness and V_f for alloy III in sulfate solution.

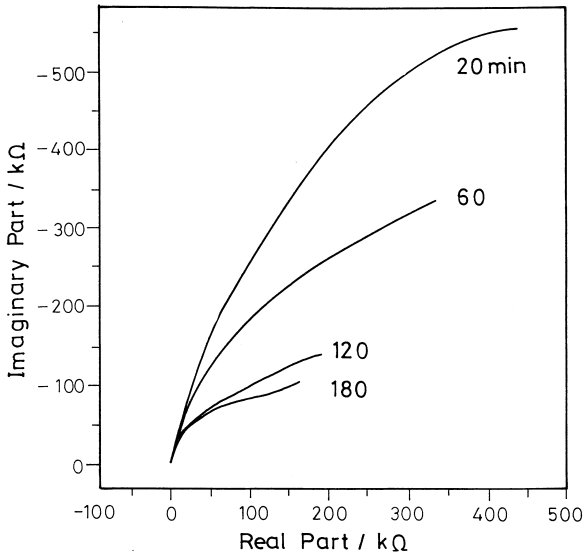

Fig. 6. Nyquist plot for alloy II in 0.1 M sulfate solutions as a function of immersion time.

overall impedance can be assumed to be negligible [9]. The plot of the reciprocals of the measured capacity and calculated values of thickness, d, produced a straight line, (Figure 4). The value of the actual double layer capacity was obtained by extrapolation of the straight line to intersect the ordinate. The value obtained for C_{dl} in tartrate medium for alloy I was 76.9 μF cm^{-2}, which is concordant with 77 μF cm^{-2} obtained for Al in borate buffer (pH 7.8) [9]. The values for alloy II and III were 31.7 and 32.4 μF cm^{-2}, respectively.

The oxide thickness value, d, was also calculated at each formation voltage. Figure 5 shows the dependence of d on V_f for alloy III after immersion in sulfate medium. The slope of the straight line produces the anodization constant which is equal to 0.098 nm V^{-1}, as compared to 0.118 nm V^{-1} obtained for Al in H_3PO_4 [1]. In tartrate solution the anodization constant for the same electrode was 0.036 nm V^{-1}, while the anodization constants for electrodes I and II in sulfate medium were 0.052 and 0.071 nm V^{-1}, respectively, which indicates that the rate of oxide growth is higher in sulfate than in tartrate solution.

3.2.3. *Kinetics of oxide layer dissolution in absence and presence of Cl^- ions*

The electrodes were anodically polarized to 15 V at a current density of 10 mA cm^{-2} in 0.1 M sodium sulfate solution. It has been reported that the Cl^- ions present in tartrate solution are removed from the electrolyte during anodization by their incorporation in the oxide film [13]. After interruption of the electric current, impedance plots were traced as a function of time in the same solution. Results for alloy II in 0.1 M sulfate solution are shown in Figure 6. The Nyquist plot indicates a decrease in R_p with time, which indicates continuous dissolution of the oxide in this medium.

Comparison of the results for the three alloys showed that after decrease of R_p for a certain time interval, it started to increase in case of alloy I and III. This is assumed to indicate that film repair overcomes film breakdown at the instant that R_p starts to increase. R_p was observed to increase after a shorter interval of immersion time in the case of alloy III as compared to alloy I, which indicates a better possibility of oxide growth in case of alloy III as compared with alloy I.

A plot of C^{-1} against $t^{1/2}$ for alloy II in sulfate solution is shown in Figure 7, where C^{-1} is taken to be directly proportional to the oxide film thickness [14]. The relation in Figure 7 is represented by:

$$C^{-1} = C_0^{-1} - \beta t^{1/2} \tag{2}$$

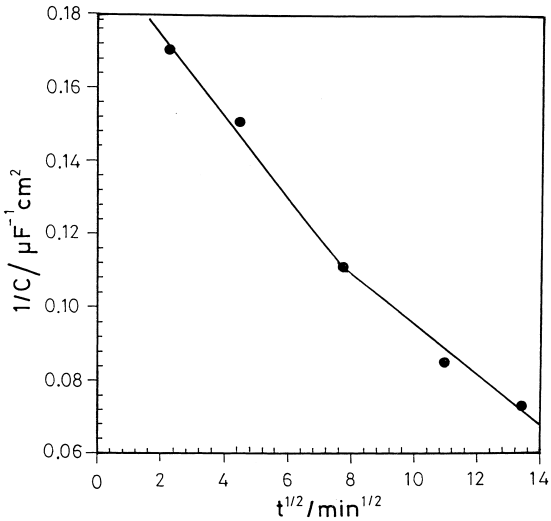

Fig. 7. Variation of the inverse of capacitance with time for alloy II in sulfate solution.

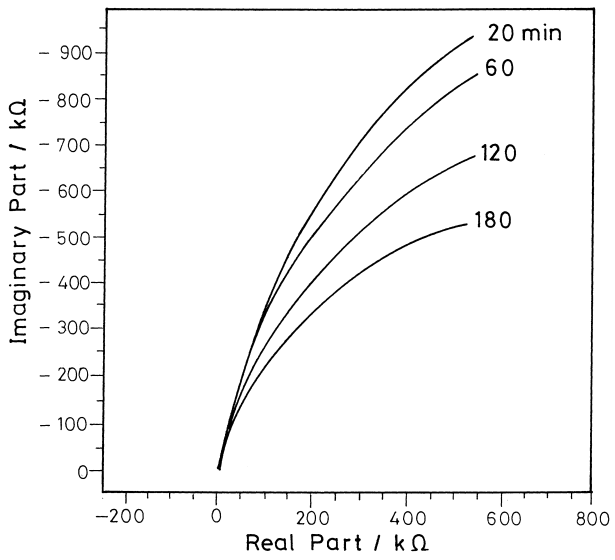

Fig. 8. Effect of time on the Nyquist plot for alloy I in presence of 10^{-3} M Cl^- in sulfate solution.

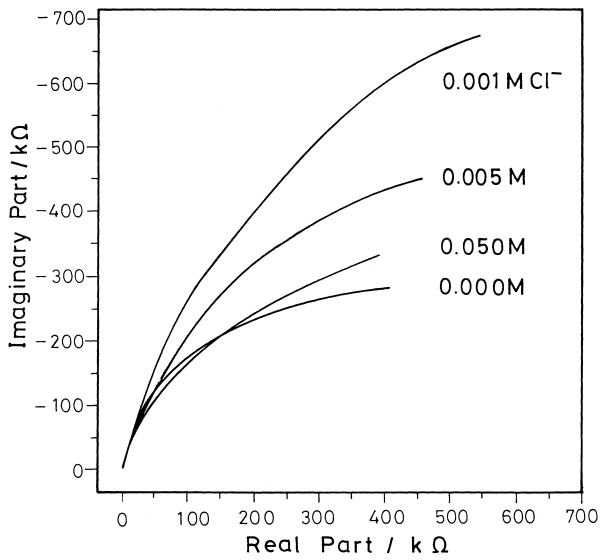

Fig. 9. Nyquist plots for alloy I showing the effect of Cl^- ion concentration in 0.1 M sulfate solution.

where C^{-1} andC_0^{-1} represent the relative oxide film thickness at time t and at zero immersion time, respectively, and β is the slope of the relation, which indicates the rate of oxide film dissolution. The relation consists of two linear parts with different β values. This indicates a decrease in the rate of dissolution after a certain time, t, which is 58 min in the present case. The decrease in the value of β indicates that the oxide consists of two layers, the outer layer being more susceptible to dissolution [15] due to the duplex nature of the porous oxide film on the Al surface [7].

Values of the rate of oxide film dissolution, β, at the early stage of dissolution in sulfate solution are 6.12, 7.39 and 3.36 μF^{-1} cm^2 $min^{1/2}$ for alloys I, II and III, respectively. This indicates that the outer porous oxide layer dissolves faster for alloy II and slowest in case of alloy III.

The presence of Cl^- ions in the dissolution medium was examined by anodically oxidizing the electrode in 0.1 M sulfate solution. When the formation voltage reached 15 V the electrode was transferred immediately to the dissolution medium and the impedance response of the system was followed with time. The dissolution medium was 0.1 M sodium sulfate solution containing different concentrations of chloride ion. Figure 8 shows the effect of time on the Nyquist plot for alloy I in the presence of 10^{-3} M Cl^{-1} in sulfate solution. With increase of immersion time, the attack by Cl^- ions is more severe, as shown by the decrease in the value of R_p.

Figure 9 shows the effect of Cl^- ion concentration on alloy I after 2 h immersion in sulfate solution. Table 6 shows the effect of both Cl^- ion concentration and immersion time on the value of R_p for alloy I in sulfate solution. It is clear that at the early stages of immersion (60 min) the rate of passive film repair is much higher than barrier layer dissolution; this has been observed before in the case of anodized Al in H_3PO_4 [1]. At this stage Cl^- ion adsorption is possible, as expected by the positive charge that should exist on aluminium at pH < 9.1 [16]. Yet, the opposite situation is observed on extended immersion and high Cl^- concentration. The Cl^- ions spread beneath the passive film through the defects in the barrier layer, leading to formation of an oxyhalide layer. This non-protective layer grows faster in the presence of high Cl^- ion concentration [1]. The rate of oxide film dissolution exceeds that of film repair, and substantial decrease in R_p is observed on extended immersion when the Cl^- ion concentration is high.

Table 6. Variation of R_p (kΩ cm^2) with [Cl^-] and time (min) for alloy I in 0.1 M sulfate solution

[Cl^-]/M	60 min	120 min	180 min
1×10^{-3}	305.1	260.0	220.7
5×10^{-3}	236.1	239.3	180.8
1×10^{-2}	192.6	193.4	141.5
5×10^{-2}	193.8	175.3	91.8
1×10^{-1}	–	112.1	–

4. Conclusion

The corrosion behaviour of the three selected Al–Si alloys in aqueous solution is complex. It depends on the pH, anion type and alloy composition. The films formed on the alloy surfaces by anodization have better protective properties than those formed naturally. The passivation of the alloys increases up to a critical potential (15–16 V) after which breakdown occurs. The presence of Cl^- ions in the dissolution medium causes severe attack of the anodically formed oxide layer, the attack being more severe at higher Cl^- ion concentration and longer immersion times.

References

1. Faiza M. Al-Karafi and Waheed Badawy, *Electrochim. Acta* **40** (1995) 1811.
2. N.A. Hampson, N. Jackson and B.N. Stirrup, *Surf. Technol.* **5** (1977) 277.
3. F. Hunkeler and H. Bohni, *Werkst. Korros.* **37** (1983) 68.
4. Seong-Min Lee and Su Il Pyun, *J. Appl. Electrochem.* **22** (1992) 151.
5. H.J.W. Lenderink, M.V.D. Linden and J.H.W. De Wit, *Electrochim. Acta* **38** (1993) 1989.
6. G. Lyberatos and L. Kobotiatis, *Corrosion* **47**(11) (1991) 820.
7. A.R. Despic, D.M. Drazic and Lj. Gajic-Krstajic, *J. Electroanal. Chem.* **242** (1988) 303.
8. G. Petermarakis and K. Moussoutzanis, *Electrochim. Acta* **40** (1995) 699.
9. S. Gudic, J. Radosevic and M. Kliskic, *J. Appl. Electrochem.* **26** (1996) 1027.
10. J.A. Bardwell and M.C.H. Mckubre, *Electrochim. Acta* **36** (1991) 647.
11. V. Rammelt and G. Reinhard, *Electrochim. Acta* **35** (1990) 1045.
12. J. Hitzig, K. Juttner, W.J. Lorenz and W. Paatsch, *Corr. Sci.* **24** (1984) 945.
13. G.S. Nadkarni, S. Radhakrishnan and S.V. Maduskar, *J. Phys D.*, **17**(1) (1984) 209.
14. E.M. Patrito, R.M. Forresi, E.M.P. Leiva and V.A. Macagno, *J. Electrochem. Soc.* **137** (1990) 527.
15. J.W. Diggle, T.C. Downie and C.W. Goulding, *Electrochim. Acta* **15** (1970) 1079.
16. B. Muller, K. Franze and D. Mebarek, *Corrosion* **51**(8) (1995) 625.